

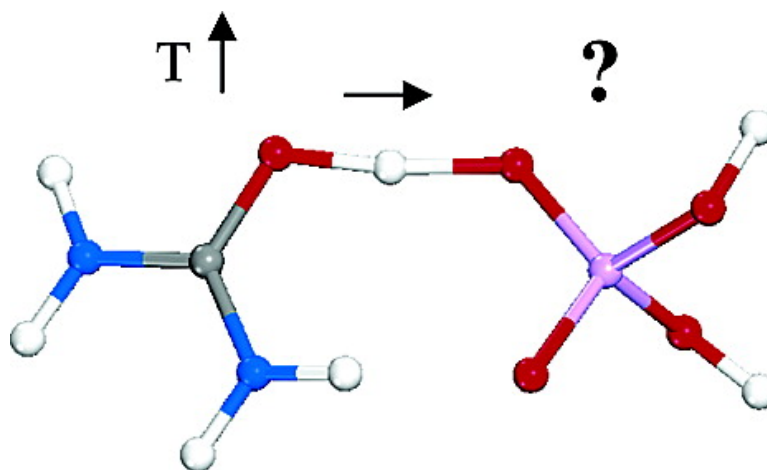
Article

Toward Understanding Mobile Proton Behavior from First Principles Calculation: The Short Hydrogen Bond in Crystalline Urea–Phosphoric Acid

Carole A. Morrison, Muhammad M. Siddick, Philip J. Camp, and Chick C. Wilson

J. Am. Chem. Soc., **2005**, 127 (11), 4042-4048 • DOI: 10.1021/ja043327z • Publication Date (Web): 25 February 2005

Downloaded from <http://pubs.acs.org> on March 24, 2009



More About This Article

Additional resources and features associated with this article are available within the HTML version:

- Supporting Information
- Links to the 7 articles that cite this article, as of the time of this article download
- Access to high resolution figures
- Links to articles and content related to this article
- Copyright permission to reproduce figures and/or text from this article

[View the Full Text HTML](#)

Toward Understanding Mobile Proton Behavior from First Principles Calculation: The Short Hydrogen Bond in Crystalline Urea–Phosphoric Acid

Carole A. Morrison,^{*,†} Muhammad M. Siddick,[†] Philip J. Camp,[†] and Chick C. Wilson[‡]

Contribution from the School of Chemistry, University of Edinburgh, West Mains Road, Edinburgh EH9 3JJ, U.K., and Department of Chemistry, University of Glasgow, University Avenue, Glasgow G12 8QQ, U.K.

Received November 5, 2004; E-mail: C.Morrison@ed.ac.uk

Abstract: The dynamics of the intermolecular short hydrogen bond in the molecular complex of urea and phosphoric acid are investigated using plane-wave density functional theory. Results indicate migration of the proton toward the center of the hydrogen bond as temperature is increased, in line with recent experimental measurements. Computed vibrational frequencies show favorable agreement with experimental measurement. An analysis of existing neutron diffraction data leads us to conclude that the effective potential well experienced by the proton is temperature-dependent. Inspired by our computations and theoretical analysis, we offer a possible explanation for the proton migration phenomenon.

1. Introduction

There is much current interest in short, strong hydrogen bonds. The possible transfer of protons through such linkages enables charge and energy to be transferred between molecules in solid chemical and biological systems and has widespread implications for issues as diverse as ferroelectrics, electrochemical processes, crystal engineering, and enzyme action.¹

In contrast to normal and weak hydrogen bonds ($X^- - H^+ \cdots Y^-$), very strong hydrogen bonds have a quasi-covalent character. In the resulting three-center four-electron bond, the H-atom is involved in two partial covalent bonds of comparable bond orders (i.e., $X-H-Y$); one possible description of the potential energy profile defining this type of hydrogen bond is as a broad, single well.² One system in which much of our recent work has focused is that of the urea–acid complexes. In these, a rich variety of short, strong hydrogen bonds is found to be present in a relatively simple framework and is therefore very suitable for in-depth study by experimental and computational methods. It is well-known that the acidic H-atom can show a varying degree of transfer from one compound (the acid) to the other (urea). In the case of the 1:1 adduct of urea and phosphoric acid (the title compound urea–phosphoric acid (UPA); see Figure 1), neutron diffraction analyses have demonstrated a situation intermediate between these two extremes, with apparent migratory behavior of the bridging hydrogen atom with tem-

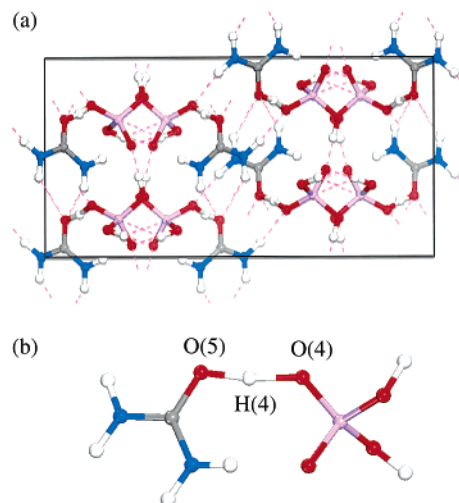


Figure 1. (a) Crystal structure of UPA. (b) One UPA dimer unit showing atom labeling scheme for the three-center, two-electron short hydrogen bond with migrating bridging proton.

perature; the proton position is found to change by some 0.05 Å toward the center of the bond as the temperature is increased from $T = 15$ K to $T = 300$ K.³

The work presented here is aimed at a deeper understanding of the short, strong hydrogen bond in the model material urea–phosphoric acid. By complementing existing experimental measurements with theoretical and computational modeling, we aim to build a more complete picture of the often subtle effects governing the description of such hydrogen bonds. We have recently published a $T = 0$ K (ground-state) plane-wave density

[†] University of Edinburgh.

[‡] University of Glasgow.

(1) (a) Steiner, T. *Angew. Chem., Int. Ed.* **2002**, *41*, 48. (b) Zundel, G. *Adv. Chem. Phys.* **2000**, *111*, 1. (c) Golubev, N. S.; Denisov, G. S.; Gindin, V. A.; Ligay, S. S.; Limbach, H.-H.; Smirnov, S. N. *J. Mol. Struct.* **1994**, *322*, 83. (d) Pan, F.; Wong, M. S.; Gramlich, V.; Bosshard, C.; Guenter, P. *Chem. Commun.* **1996**, *13*, 1557.
(2) Wilson, C. C. *Single-Crystal Neutron Diffraction from Molecular Materials*; World Scientific: Singapore, 2000.

(3) (a) Wilson, C. C.; Shankland, K.; Shankland, N. Z. *Kristallogr.* **2001**, *216*, 303. (b) Wilson, C. C. *Acta Crystallogr.* **2001**, *B57*, 435. (c) Wilson, C. C.; Morrison, C. A. *Chem. Phys. Lett.* **2002**, *362*, 85.

functional theory (PW-DFT) calculation on UPA, which, to our knowledge, was the first to produce an authentic computational description of a very short hydrogen bond in a crystal structure.^{3c} The calculations reproduced the short asymmetric hydrogen bond with the proton partly transferred to urea [$r\text{O}(4)\cdots\text{O}(5) = 2.425 \text{ \AA}$, $r\text{H}(4)\cdots\text{O}(5) = 1.11 \text{ \AA}$; cf. neutron diffraction ($T = 15 \text{ K}$) $2.416(2) \text{ \AA}$, $1.158(4) \text{ \AA}$], in sharp contrast to the optimized structure obtained from isolated-molecule calculations based on a UPA dimer model, which implied a hydrogen bond that neither was short [$r\text{O}(4)\cdots\text{O}(5) = 2.60 \text{ \AA}$] nor showed any evidence of proton transfer [$r\text{H}(4)\cdots\text{O}(5) = 1.00 \text{ \AA}$], clearly at odds with the experimental data. While establishing the importance of periodic boundary conditions in obtaining the correct geometry for the solid state was in itself an important result, it was also clearly important to then carry the calculations forward and model (and thus explain) the effects of temperature on the crystal structure. To this end, we have now undertaken a series of PW-DFT molecular dynamics (MD) calculations to ascertain whether the simulations can correctly reproduce the migratory proton behavior and its temperature dependence and, if so, help shed light on why these structural changes take place. Furthermore, by performing a Fourier transformation of the calculated forces of the atoms, we can also obtain the vibrational frequencies for the unit cell model that will be automatically corrected for anharmonicity, crucial for the correct description of short hydrogen bond systems.

For any discussion concerned with the mobility of bridging protons in short hydrogen bonds, some time must be devoted to the nature of the potential energy surface (PES) itself. As mentioned above, these potentials are often, but not exclusively, regarded as being broad single wells.² For proton migration to occur, two scenarios are possible. The effective potential may be unresponsive to temperature and thus an increase in thermal energy simply allows the proton to sample higher-energy states. In an alternate scenario, the shape of the effective potential is dependent on temperature, and the proton lies in the lowest-energy state appropriate for that temperature. To address this central issue, we have modeled the extensive previously published variable temperature neutron diffraction results³ to establish whether the nature of the potential is dependent on temperature.

In this article, we report the results obtained from four PW-DFT molecular dynamics simulations carried out for UPA at $T = \text{ca. } 40, 125, 225, \text{ and } 340 \text{ K}$. The change in geometry for the short hydrogen bond as a function of temperature is discussed before considering the calculated vibrational spectra. We also report on the temperature dependence of the PES for UPA by theoretically modeling existing neutron diffraction data. Finally, we offer a possible explanation for the mobile proton behavior.

2. Model and Theoretical Methods

The crystal structure of urea–phosphoric acid belongs to the orthorhombic space group $Pbca$ with lattice parameters $a = 17.401 \text{ \AA}$, $b = 7.428 \text{ \AA}$, and $c = 8.903 \text{ \AA}$ (neutron diffraction, $T = 15 \text{ K}$), giving eight dimer units in the unit cell. The urea and phosphoric acid molecules are stacked in alternate layers and link together by a complicated network of hydrogen bonding (see Figure 1). The phosphoric acid molecules link through standard hydrogen bonds ($r\text{O}\cdots\text{O} = 2.576 \text{ and } 2.636 \text{ \AA}$), while between urea and phosphoric acid two different interactions exist: a weak hydrogen bond via a $\text{N}\cdots\text{O}$ linkage (2.880 \AA) and a very short hydrogen bond via an $\text{O}\cdots\text{O}$ linkage

(2.417 \AA). It is this last bond that displays proton mobility with temperature and forms the primary interest in this research.

2.1. Molecular Dynamics Calculations. A series of PW-DFT microcanonical (NVE) molecular dynamics calculations have been carried out for the unit cell of urea–phosphoric acid using the VASP 4.4 simulation code.⁴ A generalized gradient approximation (PW91) was used for the exchange and correlation potential.⁵ The wave function was generated using a series of pseudopotentials and delocalized plane waves expressed at an energy cutoff of 297 eV . Integrations over the Brillouin zone were performed using one k -point at the Γ position.

In total, four simulations were performed with equilibrated temperatures of approximately $40, 125, 220, \text{ and } 340 \text{ K}$. A time step of 0.75 fs was chosen to enable appropriate sampling of the highest vibrational frequency in our system, namely the NH_2 stretching mode. This was found to be an appropriate value following subsequent careful monitoring of energy conservation in the NVE ensemble. Simulations were run for 0.6 ps , with the first 0.2 ps worth of data discarded to ensure the system had reached equilibrium. The highest temperature simulation was run for a further 0.1 ps to verify that no further changes out with one or two uncertainty ranges in the averaged structure parameters recorded in Table 1 occurred. Vibrational frequencies were obtained by Fourier transformation of the autocorrelation function of the calculated forces; low-frequency noise was subtracted from the Fourier transforms using a Blackman windowing function.⁶

In the simulations reported here the input geometry was taken from our previously reported equilibrium structure, in which both lattice vectors and atomic positions were optimized until convergence was achieved. This structure reproduced the experimental lattice vectors to within 0.15 \AA , all intramolecular bond distances to within 0.02 \AA , and angles to within 1° .^{3c}

3. Asymmetric Hydrogen Bond

3.1. Neutron Diffraction. $\text{O}(5)\cdots\text{H}(4)\cdots\text{O}(4)$ bond lengths in the temperature range $15 \leq T \leq 335 \text{ K}$ as obtained by neutron diffraction are reported in Table 1 and plotted in Figure 2. As the $\text{O}\cdots\text{H}\cdots\text{O}$ linkage is very close to linear (see Figure 1b), for what follows it is convenient to define the quantities σ and δ as half the sum and difference, respectively, of the $\text{O}(4)\cdots\text{H}(4)$ and $\text{O}(5)\cdots\text{H}(4)$ bond lengths; that is,

$$\sigma = \frac{1}{2}[r\text{O}(4)\cdots\text{H}(4) + r\text{O}(5)\cdots\text{H}(4)] \quad (1)$$

and

$$\delta = \frac{1}{2}[r\text{O}(4)\cdots\text{H}(4) - r\text{O}(5)\cdots\text{H}(4)] \quad (2)$$

From the experimental results in Table 1, σ is only very weakly dependent on temperature, the weighted average value being $\sigma = 1.2128(11) \text{ \AA}$ (throughout this article, the number in parentheses represents the estimated statistical uncertainty in the final digits). By contrast, δ shows strong temperature dependence, as shown in Figure 2a; the corresponding bond lengths are shown in Figure 2b. At temperatures below $T \approx 315 \text{ K}$, the difference parameter $\delta > 0$, which reflects a preference of $\text{H}(4)$ for proximity to $\text{O}(5)$ rather than $\text{O}(4)$; above this temperature, δ is effectively zero within statistical uncertainties.

(4) Kresse, G.; Furthmüller, J. *Comput. Mater. Sci.* **1996**, *6*, 15.

(5) Perdew, J. P.; Chevary, J. A.; Vosko, S. H.; Jackson, K. A.; Singh, D. J.; Fiolhais, C. *Phys. Rev. B* **1992**, *46*, 5571.

(6) Allen, M. P.; Tildesley, D. J. *Computer Simulation of Liquids*; Clarendon Press: Oxford, 1987.

Table 1. Bond Lengths and the Parameters σ (1) and δ (2) as Functions of Temperature as Obtained from Neutron Diffraction [3] and MD Simulations^a

T/K	rO(4)···O(5)	rO(4)···H(4)	rO(5)···H(4)	σ	δ
Neutron Diffraction [Average $\sigma = 1.2128(11)$ Å]					
15	2.4165(20)	1.267(4)	1.158(4)	1.2125(28)	0.0545(28)
150	2.412(2)	1.252(4)	1.168(4)	1.2100(28)	0.0420(28)
250	2.405(6)	1.237(9)	1.176(10)	1.2065(67)	0.0305(67)
280	2.417(7)	1.240(11)	1.195(12)	1.2175(81)	0.0225(81)
290	2.403(6)	1.235(10)	1.179(11)	1.2070(74)	0.0280(74)
295	2.420(7)	1.252(10)	1.180(11)	1.2160(74)	0.0360(74)
300	2.422(6)	1.238(10)	1.193(11)	1.2155(74)	0.0225(74)
305	2.422(7)	1.231(10)	1.199(11)	1.2150(74)	0.0160(74)
310	2.431(7)	1.239(10)	1.201(11)	1.2200(74)	0.0190(74)
315	2.433(7)	1.219(11)	1.221(11)	1.2200(78)	-0.0010(78)
320	2.425(8)	1.222(11)	1.214(12)	1.2180(81)	0.0040(81)
330	2.419(8)	1.221(12)	1.208(13)	1.2145(88)	0.0065(88)
335	2.430(9)	1.226(15)	1.214(15)	1.220(11)	0.006(11)
Molecular Dynamics [Average $\sigma = 1.2259(28)$ Å]					
0	2.425	1.328	1.106	1.2170	0.1110
39.9(1)	2.4377(4)	1.3326(8)	1.1159(5)	1.2243(5)	0.1084(5)
127.2(4)	2.4373(6)	1.3066(14)	1.1440(12)	1.2253(9)	0.0813(9)
225.2(6)	2.4412(8)	1.3023(18)	1.1563(15)	1.2293(12)	0.0730(12)
337.0(9)	2.4467(9)	1.2769(22)	1.1901(20)	1.2335(15)	0.0434(15)

^a All bond lengths are in angstroms.

3.2. Molecular Dynamics. The geometry changes recorded in the MD simulations for the short hydrogen bond in crystalline UPA (averaged over all eight dimer units) are given in Table 1, alongside experimental parameters and the previously reported equilibrium structure for direct comparison. Like the neutron diffraction results, the simulations also describe an asymmetric bond with the bridging hydrogen migrating from urea toward the center of the bond as the temperature rises. The simulated bridge is slightly more asymmetric than what was found experimentally, and at present the reason for this discrepancy is unclear. The differences are evident in Figure 2, where the experimental and calculated values of δ , $rO(4) \cdots H(4)$, and $rO(5) \cdots H(4)$ are plotted together for direct comparison. Like the experimental data, σ shows no strong systematic variation with temperature (1% increase between $T = 0$ K and $T = 337$ K) and hence to a first approximation is considered constant and equal to the average value $\sigma = 1.2259(28)$ Å, this being only 1% larger than the corresponding experimental value.

The migratory proton behavior observed in the MD simulations is shown graphically in Figure 3, where the change in $rO(4) \cdots O(5)$, $rO(4) \cdots H(4)$, and $rO(5) \cdots H(4)$ over time for one of the UPA dimer units in the crystal lattice is displayed. From this it can be seen that $rO \cdots O$ is essentially constant over the duration of the simulation [average value 2.437(4) Å compared to 2.419(1) Å by experiment], with greater variation in the highest temperature simulation. Some fluctuation should be expected in all measured parameters, however, as the sample size (one unit cell = 128 atoms) is statistically quite small. If the simulations were repeated with a larger unit cell (e.g., a $2 \times 2 \times 2$ lattice) then these oscillations would diminish, but at great computational cost. The MD geometry plots also nicely demonstrate the proton mobility over the course of the simulations: proton motion clearly increases with temperature, and at high temperature the bridging atom makes it past the midpoint of the $O \cdots O$ bond (1.2 Å), shuttling between urea and phosphoric acid. The dynamics of the short hydrogen bond is also agreeably demonstrated in a multiplicity plot of δ (expressed to two decimal places) obtained for all eight hydrogen bonds in the unit cell for the four MD simulations (Figure 4).

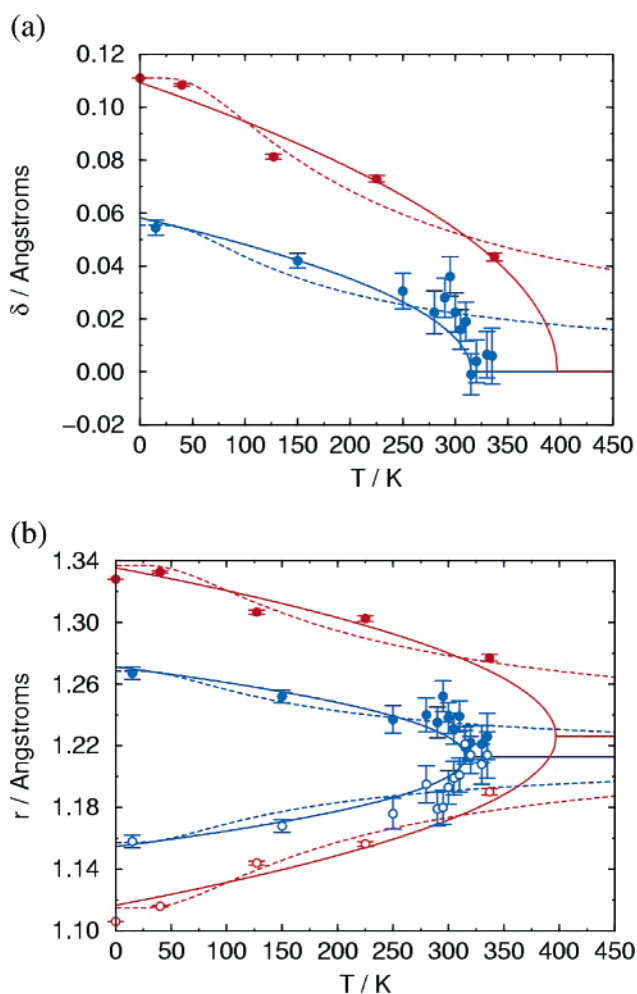


Figure 2. (a) Thermal average of δ as a function of temperature from neutron diffraction (solid blue points), MD simulations (solid red points), a harmonic-oscillator theory (eq 3) (dashed curves), and a phenomenological mean-field theory (eq 5) (solid curves). (b) Thermal averages of the $O(4) \cdots H(4)$ and $O(5) \cdots H(4)$ bond lengths from neutron diffraction (solid and open blue points, respectively), MD simulations (solid and open red points, respectively), a harmonic-oscillator theory (dashed curves), and a phenomenological mean-field theory (solid curves).

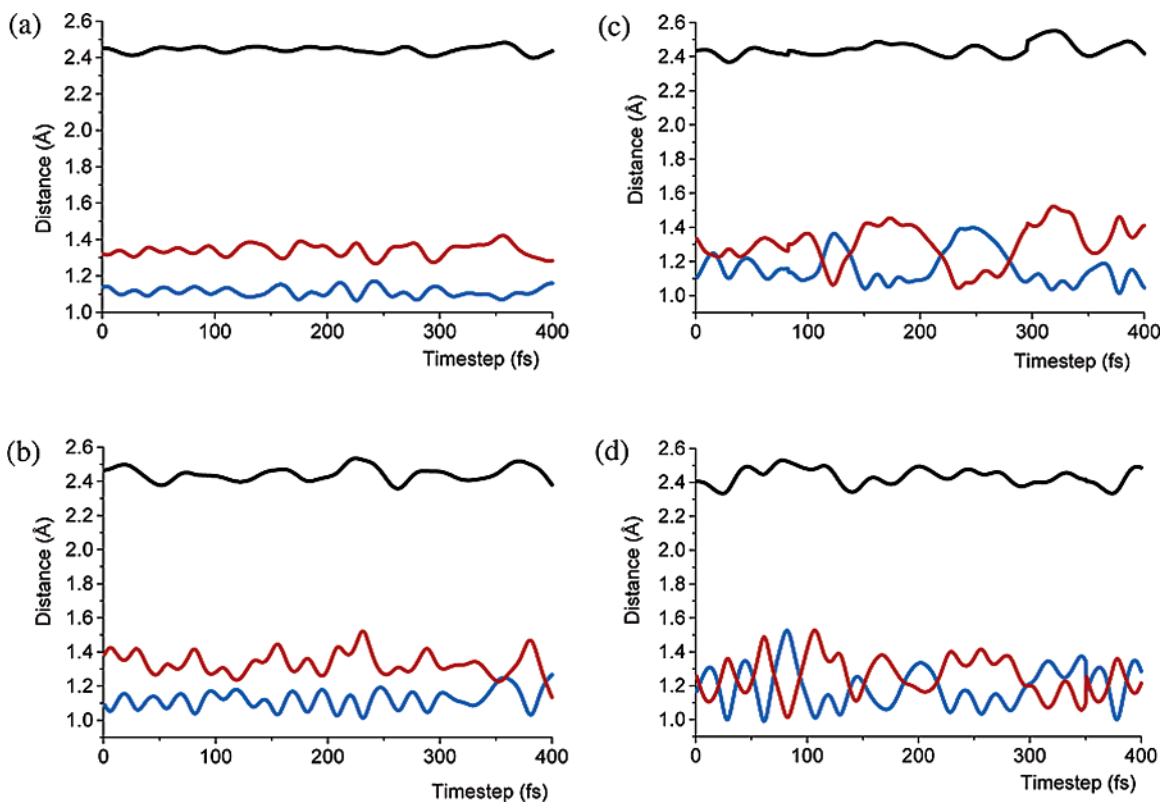


Figure 3. Geometries obtained for the short hydrogen bond in UPA by MD simulation: (a) 39.9(1), (b) 127.2(4), (c) 225.2(6), and (d) 337.0(9) K [black $rO\cdots O$, red $rO(4)\cdots H(4)$, blue $rO(5)\cdots H(4)$]. Time intervals are 0.75 fs.

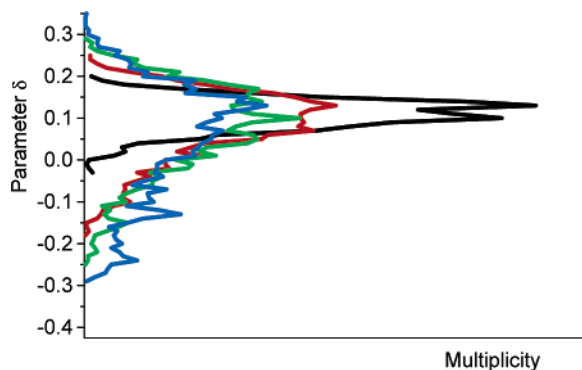


Figure 4. Multiplicity plots of δ (expressed to two decimal places) for the unit cell of UPA [black 39.9(1), red 127.2(4), green 225.2(6), and blue 337.0(9) K].

From this it is verified that at 39.9(1) K the protons spend most time approximately 0.1 Å away from the middle of the $O\cdots O$ bond toward urea. At higher temperatures, the protons are able to explore more of the hydrogen bond potential, and although they spend a significant amount of time close to phosphoric acid, they are statistically more likely to be found close to urea in the same position as in the low-temperature simulation. At 337 K, the time scale for proton migration is on the order of 15 fs, comparable with that obtained in a molecular dynamics study for the short intramolecular hydrogen bond in benzoylacetone.⁷

3.3. Phenomenological Theory. The temperature dependence of δ illustrated in Figure 2a could arise through one of two general types of mechanisms that are discussed below. First, the temperature dependence might arise simply from the thermal

population of excited states. For the purposes of illustration, it is assumed that the energy levels of a given proton are those of harmonic oscillator, that is, $E_n = (n + 1/2)\hbar\omega$ with $n = 0, 1, 2, \dots$, which might arise when the proton is localized in one of the wells of a double-well potential. In the current scenario, it is also assumed that at low temperatures the thermal average of δ will be dominated by contributions from the ground state with a quantum-mechanical expectation value $\langle 0|\hat{\delta}|0\rangle > 0$, in accord with the experimental results. At higher temperatures, the thermal average will contain contributions from excited states with expectation values assumed to be equal to zero, that is, $\langle n|\hat{\delta}|n\rangle = 0$ for $n = 1, 2, 3, \dots$. In this scenario, the thermal average of δ is given by

$$\delta(T) = \langle 0|\hat{\delta}|0\rangle [1 - \exp(-\Theta/T)] \quad (3)$$

where $\Theta = \hbar\omega/k_B$ is a vibrational temperature. Equation 3 has been fitted separately to the experimental results [$\Theta = 153(29)$ K, $\delta(0) = \langle 0|\hat{\delta}|0\rangle = 0.0555(44)$ Å] and the MD results [$\Theta = 178(24)$ K, $\delta(0) = 0.1109(66)$ Å]. The resulting curves are plotted in Figure 2a, while $rO(4)\cdots H(4) = \sigma + \delta(T)$ and $rO(5)\cdots H(4) = \sigma - \delta(T)$ are shown in Figure 2b. It is clear that the temperature dependence in this scenario is not consistent with the results obtained from neutron scattering, particularly at high temperatures. Equation 3 is only barely adequate in fitting the results from the MD simulations. It is anticipated that related models, with different energy levels and expectation values, would yield similar types of curves.

It will now be shown that the experimental and simulations results are consistent with there being a mean field experienced by each proton that varies with temperature. The inspiration for this theory is the observation that at low temperatures $\delta >$

(7) Pantano S.; Alber F.; Carloni, P. *J. Mol. Struct. (THEOCHEM)* **2000**, *530*, 177.

0, while at high temperatures δ is essentially zero. Hence, δ plays the role of an “order parameter” for a symmetry-breaking phase transition that occurs at some critical temperature, T_C . The simplest phenomenological theory of phase transitions, Landau theory,⁸ involves writing the temperature-dependent *thermodynamic* potential as a polynomial expansion in δ :

$$f = f_0 + \frac{1}{2}f_2\Delta T\delta^2 + \frac{1}{4}f_4\delta^4 \quad (4)$$

where $\Delta T = T - T_C$ and $f_2, f_4 > 0$. This function describes a symmetric, double-well potential with its minima at $\delta \neq 0$ when $\Delta T < 0$, and a single-well potential with its minimum at $\delta = 0$ when $\Delta T \geq 0$. The thermal average of δ is therefore identified with its (positive) value at the global minimum of the potential; that is,

$$\delta(T) = \begin{cases} \sqrt{\frac{f_2\Delta T}{f_4}} & T < T_C \\ 0 & T \geq T_C \end{cases} \quad (5)$$

Fitting eq 5 to the experimental results for δ yields the parameters $T_C = 315(2)$ K, $f_2/f_4 = 1.08(11) \times 10^{-5} \text{ K}^{-1} \text{ \AA}^2$, and $\delta(0) = \sqrt{f_2 T_C / f_4} = 0.0583(30) \text{ \AA}$; the fits are shown in Figure 2a. In Figure 2b, the experimental bond lengths are compared with curves derived from the fits with $\sigma = 1.2128(11) \text{ \AA}$. Clearly, the experimental results are consistent with the hydrogen being confined to the heuristic temperature-dependent potential in eq 4.

The results from MD simulations have also been fitted using eq 5, yielding the parameters $T_C = 397(20)$ K, $f_2/f_4 = 3.01(30) \times 10^{-5} \text{ K}^{-1} \text{ \AA}^2$, and $\delta(0) = 0.1093(61) \text{ \AA}$; the corresponding fits are shown in Figure 2a. In Figure 2b, the bond lengths from MD simulations are compared with curves derived from the fits with $\sigma = 1.2259(28) \text{ \AA}$. The values of T_C , f_2/f_4 , and $\delta(0)$ are all larger than the corresponding values obtained from the experimental results by factors of 1.3, 2.8, and 1.9, respectively. The agreement is at least within an order of magnitude, however, and this should be taken as an encouraging sign that the phenomenological theory is consistent with both experiment and MD simulation.

In principle, eq 4 could contain linear and/or cubic terms to capture any asymmetry that may exist in the potential. In practice, including these terms offered no significant improvement to the fits, and the corresponding coefficients were essentially zero within the statistical uncertainties. This could be taken to mean that the asymmetry in the potential is weak; however, it should be noted that our fits are based on measured values of $\delta \geq 0$ only, and hence we have no direct information regarding the $\delta < 0$ portion of the potential.

4. Vibrational Spectra from Molecular Dynamics

In general, our calculated set of vibrational frequencies obtained from the MD simulations proved to be an excellent match with the experimental variable-temperature IR/R study of Barnes et al.,⁹ with many of our signals within 1–2% of the

Table 2. Selected UPA Experimental and Calculated Vibrational Frequencies (cm^{-1})

IR (20 K)	calcd [39.9(1) K]	IR (310 K)	calcd [337.0(9) K]	assignment
3450	3510	3450	3430	$\nu_{\text{as}}(\text{NH}_2)$
3320	3285	3320	—	$\nu_{\text{s}}(\text{NH}_2)$
1900–2800	max. 2725	1900–2880	max. 2790	$\nu(\text{O}-\text{H}\cdots\text{O})$
1670	1665	1660	1650	$\nu(\text{CO})$
1640	1645	1630	1650	$\delta(\text{NH}_2)$
1515	1660	—	1715	$\delta(\text{O}\cdots\text{H}\cdots\text{O})$
1580	1590	1560	1600	$\delta(\text{NH}_2)$
—	1460	—	1390	$\gamma(\text{O}\cdots\text{H}\cdots\text{O})$
1230	1225	1210	1240	$\delta(\text{O}-\text{H}\cdots\text{O})$
1190	1020	1170	1020	$\delta(\text{NH}_2)$
—	1100	—	1120	$\nu_{\text{as}}(\text{O}\cdots\text{H}\cdots\text{O})$
890–995	max. 900	890–995	max. 900	$\nu(\text{PO})$
872	975	875	910	$\gamma(\text{O}-\text{H}\cdots\text{O})$

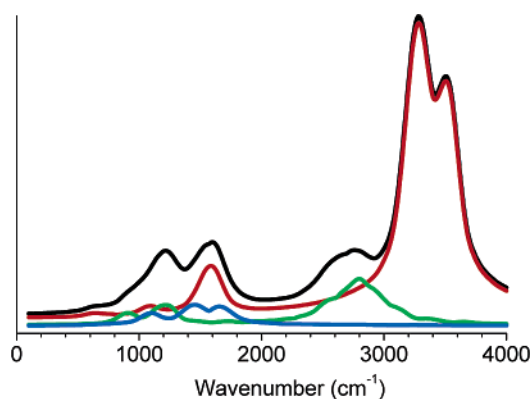


Figure 5. Calculated vibrational spectrum for UPA at 40 K (hydrogen atoms only, black all H atoms, red NH_2 only, green (PO)H only, and blue short bridging H only).

experimental wavenumbers (see Table 2; IR values quoted only for ease of comparison).

While it is not possible to analyze individual modes, as with a normal-mode analysis, Fourier transformation of the autocorrelation function of the forces for selected groups of atoms allowed the main features of the spectra to be identified. An example of the plots obtained from the lowest temperature simulation (ca. 40 K) is given in Figure 5, where the black lines are the signals obtained for all hydrogen atoms, the red lines are for the NH_2 hydrogen atoms only, green lines show the hydrogen atoms associated with the phosphoric acid OH groups not involved with the short hydrogen bond linkage (i.e., standard hydrogen bonding), and the blue lines are those associated with the short bridging migratory H atoms only (see Supporting Information for other element plots). Hence, although we cannot positively identify the symmetry coordinates for each peak in the spectra, we can block out regions of the spectra to particular groups of atoms or functional groups. In the lowest temperature spectrum we can clearly see two peaks for the NH_2 hydrogen atoms at approximately 3510 and 3285 cm^{-1} (see Figure 6a), which we can confidently assign to the asymmetric and symmetric stretching modes, respectively. In the highest temperature simulation (ca. 335 K), these bands shift closer together and appear to coalesce in a broad peak with maxima 3430 cm^{-1} . The infrared reported values appear to be unaffected by the change in temperature, but at 3450 and 3320 cm^{-1} agree very favorably with our computed values.

The standard hydrogen bonds linking phosphoric acid molecules together (see Figures 1a and 6b) give rise to a series of

(8) Chaikin, P. M.; Lubensky, T. C. *Principles of Condensed Matter Physics*; Cambridge University Press: Cambridge, 1997.

(9) Iliczyszyn, M. M.; Ratajczak, H.; Barnes, A. J. *J. Raman Spectrosc.* **1992**, *23*, 1.

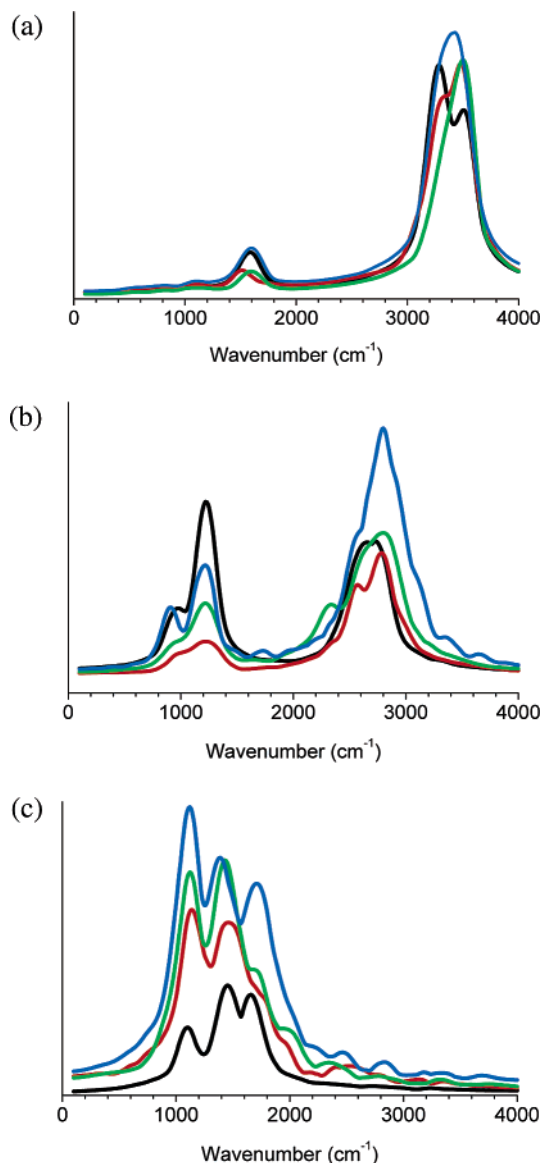


Figure 6. Calculated vibrational spectrum for UPA H atoms only (a) NH_2 , (b) POH standard H bonded atoms, (c) short bridging H atoms. [black 39.9-(1), red 127.2(4), green 225.2(6), and blue 337.0(9) K].

broad peaks between 2300 and 3000 cm^{-1} (maxima 40 K: 2725 cm^{-1} ; 335 K: 2790 cm^{-1}), which reside in the region traditionally attributed to hydrogen bond stretching modes and is broadly consistent with the experimental assignments. A series of sharper peaks, presumably the in- and out-of-plane bending modes, at 1225, 975 (40 K), 1240, and 910 cm^{-1} (335 K) closely match the experimental values (see Table 2).

The three short bridging modes calculated to lie at 1660, 1460, 1100 cm^{-1} (40 K) and 1715, 1390, and 1120 (335 K) (Table 2, Figure 6c) are not, however, wholly consistent with experiment. The IR/R signals would be expected to be very weak, making their assignment difficult: the almost linear $\text{O}\cdots\text{H}\cdots\text{O}$ linkage tends toward symmetric as temperature is increased, resulting in a weak (and decreasing) dipole or polarizability change. Additional coupling between modes with a strong anharmonic potential would be expected to further complicate the spectrum. Barnes tentatively assigned the $\text{O}\cdots\text{H}\cdots\text{O}$ in-plane (δ) bending mode to 1550–1500 cm^{-1} , the out-of-plane (γ) bend in the region 900–600 cm^{-1} , and the asymmetric stretch as giving

rise to a complex splitting pattern [due to strong coupling with $\nu_s(\text{O}\cdots\text{O})$] in the low-frequency region 800–300 cm^{-1} . Fillaux et al.¹⁰ also observed complex anharmonic coupling in an inelastic neutron scattering study of potassium hydrogen maleate which also contains a short (although in this case intramolecular) $\text{O}\cdots\text{H}\cdots\text{O}$ bond. They reported the in-plane (δ) and out-of-plane (γ) bends at 1650 and 1250 cm^{-1} and a complex asymmetric stretching mode (ν_a) that splits into multiple components over the region 1300–500 cm^{-1} , all of which is comparable to our calculated values for UPA. In assigning our three calculated bands for the $\text{O}\cdots\text{H}\cdots\text{O}$ linkage, we support Barnes's assignment of the strong peak recorded on the 20 K spectra at approximately 1510 cm^{-1} as the in-plane bend. Although we are overestimating the experimental assignment by some 10% (see Table 2), given that we know that our calculated geometry overestimates the asymmetry of the $\text{O}\cdots\text{H}\cdots\text{O}$ bond by a factor of 2, a 10% error margin is in all likelihood to be expected. Our prediction for the out-of-plane bend to appear at about 1460 cm^{-1} (40 K) has no obvious match with an experimental band in this region, but we must take into account the weak nature of the signal. Finally, we propose our third calculated peak (ca. 1100 cm^{-1}) to be the asymmetric stretch, which finds consistency with Fillaux's work, and is also in the right ballpark for the IR/R study of Barnes. It is also consistent with spectroscopic and computational studies of the triatomic bihalide anion $[\text{FHF}]^-$, which showed that the stretching frequency for a short, strong bond broadly similar to our $\text{O}-\text{H}-\text{O}$ system can be extremely low.¹¹ Finally, it is also of a similar magnitude to a recent computational study of the short intramolecular $\text{O}\cdots\text{H}\cdots\text{O}$ bond in picolinic acid.¹²

5. Discussion

If the PW-DFT MD simulations are indeed mimicking the experimental PES for UPA adequately enough, then it stands to reason that the explanation for proton mobility must be present in our calculated spectra. Our spectra are free from selection rule constraints, giving rise to very weak signals and, of course, the overtone and combination bands that would add a significant level of complexity to the experimental spectra of a strongly hydrogen bound system. Our data also allow us to make block assignments of regions of the spectra to different groups of atoms. Taken together, this greatly simplifies the analysis of the vibrational assignments. But it should also be remembered that there are limitations in our calculations. For instance, the optimized volume for the unit cell used in the MD simulations was obtained from the equilibrium (i.e., 0 K) structure. Since the cell would be expected to expand slightly on heating, the simulation is effectively performed at higher than ambient pressure. This would presumably have an effect on the measured vibrational frequencies. It should also be remembered that the calculations have at their heart density functional theory, with all the known limitations that this method poses. Calculations therefore do not model dispersion forces and refer to the electronic ground state at all times. But this argument can also be turned on its head: despite the limitations in our simulation, our data do support proton migration with temperature, albeit to a slightly lesser degree than measured

(10) Fillaux, F.; Leygue, N.; Tomkinson, J.; Cousson, A.; Paulus, W. *Chem. Phys.* **1999**, *244*, 387.

(11) Kawaguchi K.; Hirota, E. *J. Chem. Phys.* **1987**, *87*, 6838.

(12) Panek, J.; Stare J.; Hadži, D. *J. Phys. Chem. A* **2004**, *108*, 7417.

experimentally. Some explanation for this phenomenon must therefore be tantalizingly locked up in our simulated data.

To this end, analysis of the calculated vibrational spectra yields patterns that may (or may not) be coincidental. The highest bridging mode shifts from 1660 to 1715 cm^{-1} as the temperature is increased (see Figure 6c). This high-temperature bridging mode will have a first overtone band of 3430 cm^{-1} , which is exactly degenerate with the calculated high-temperature NH_2 stretch (see Figure 6a). Similarly, the second bridging mode shifts from 1460 to 1390 cm^{-1} ; the first overtone of this band is coincidental with the maxima of the broad O–H standard hydrogen bond stretch at 337 K (see Figure 6b). It is tempting to speculate that the reason for proton migration could be attributed to subsequent couplings between these modes. At present, we cannot comment further on the nature of this possible interaction, that is, whether there is a sudden shift in geometry as the frequencies approach degeneracy or whether the effect is a slow, steady drift. This analysis would require many more MD data points, or an appreciable reduction in the error bars quoted in the experimental data.

6. Conclusions

In this article, we have demonstrated that the PES obtained from experimental data for the short hydrogen bond in UPA is temperature-dependent. We have reported results obtained for four PW-DFT MD calculations that also support proton migration. On the basis of calculated vibrational spectra obtained from the simulations, we suggest that a possible explanation for the proton migration effect is due to coupling between the first overtone bands of the in-plane and out-of-plane bridging modes

with the NH_2 stretch and O–H standard hydrogen bond stretch, respectively.

Although the experimental variable temperature spectra have been available in the literature for some time, the bridging proton vibrational modes are too weak in intensity to be assigned experimentally with much degree of confidence. This possible explanation could therefore only be obtained from theory. Although we cannot definitively show that our tentative model for proton transfer is supported by the experimental frequency assignments for UPA, we can turn to other related systems, such as the deuterated analogue to see if that too shows proton migration. This work is currently underway.

Acknowledgment. C.A.M. is grateful to The Royal Society for the award of a University Research Fellowship and to the University of Edinburgh, School of Chemistry, for funding. M.M.S. is grateful to the University of Edinburgh (Schools of Chemistry and Physics) for the award of a Research Studentship. We thank Dr. C. R. Pulham and Dr. D. R. Allan (School of Chemistry, University of Edinburgh) for helpful discussion during the preparation of this manuscript. This work was carried out using computational facilities supplied by EPCC at the University of Edinburgh.

Supporting Information Available: Calculated vibrational spectra obtained for non-hydrogen elements in UPA and complete set of coordinate files (RTF format) obtained in the four MD runs reported in this article. This material is available free of charge via the Internet at <http://pubs.acs.org>.

JA043327Z